等离子熔覆制备 Fe_3Al 金属间化合物的组织结构

朱冬妹[1,2]， 王惜宝[2]
（1. 北京星航机电设备厂，北京 100074；
2. 天津大学 材料科学与工程学院，天津 300072）

朱冬妹

摘 要：为了提高钢铁表面的抗高温腐蚀性能，应用电弧喷涂和等离子弧熔覆方法在碳钢表面制备 Fe-Al 金属间化合物涂层。通过对熔覆层及其与钢基体界面的组织结构分析，认为该方法可以在钢基表面获得致密、无夹杂的铁铝金属间化合物层，合金层与基体间完全冶金结合；熔覆层主要由 Fe_3Al，FeAl 和 α-Fe 相构成。在试验条件下所获得的铁铝合金层，其最高显微硬度可达到 514 HV。

关键词：等离子熔覆；Fe_3Al；金属间化合物
中图分类号：TG455 文献标识码：A 文章编号：0253－360X(2008)12－0017－03

0 序 言

Fe_3Al 金属间化合物具有比重小、强度和弹性模量高、抗氧化、抗硫化、耐热腐蚀、耐磨损等一系列优异的性能特点。金属间化合物由于原子间金属键与共价键的共存性，使其可能具有金属和陶瓷的性能特点。作为高技术结构材料，Fe_3Al 金属间化合物近年来成为材料研究最活跃的领域之一[1,2]。

Fe_3Al 材料应用的主要障碍之一来源于 Fe_3Al 的脆性特征，故使其材料的应用受到较大限制。以韧性材料为基体，用 Fe_3Al 为表面涂覆材料的工艺方法制备新材料成为研究热点之一。目前在 Fe_3Al 涂层材料的热喷涂研究上有了一定进展，该方法的主要缺点是涂层薄，且与界面非冶金结合[3]。在 Fe_3Al 涂层上也有人采用了激光熔覆法[4]，该方法的主要缺点是涂层薄，设备维护成本较高。而等离子熔覆工艺过程简单，设备成本低，覆层与基体界面易实现冶金结合，热源能量密度高，是实现材料表面熔覆的一种经济灵活的热源，因此这种方法很有发展前景。

1 试验方法

试验采用的试板为 200 mm×40 mm×8 mm 的 Q235 钢板，钢板表面采用喷砂进行除锈处理。除锈处理后用 φ3.0 mm 的纯铝丝经过电弧喷涂在钢板表面制备成厚度约为 100 μm 的铝层。然后利用等离子弧对涂铝层表面进行重熔处理，通过铁基和铝层之间的高温冶金反应，在熔覆过程中原位合成 Fe-Al 金属间化合物。等离子弧熔覆参数见表 1。

表 1 等离子粉末堆焊工艺参数

Table 1 Operation parameters of plasma transferred arc

焊接电流 I/A	转移弧电压 U/V	离子气流量 q_v/L·min^{-1}	焊枪摆幅 W/mm	焊接速度 v/(mm·min^{-1})
60～160	20～40	0.4	1.6	44～160

把上述试验条件下的熔覆合金制成金相试样，分别在金相显微镜、扫描电镜下观察合金层及结合区组织结构。利用能谱仪对重点组织进行微区成分分析，并采用 X 射线衍射方法对合金层块状平面试样进行物相鉴定。利用显微硬度仪测定熔履层硬度，分析等离子熔覆 Fe_3Al 工艺条件下熔覆合金层的组织结构特点。

2 试验结果与分析

2.1 熔覆合金层的显微组织

在上述工艺条件下，等离子熔覆的表面成形如图 1 所示，从图中可以看出熔敷层表面致密、无咬边和裂纹、无肉眼可见气孔、夹杂等缺陷。图 2 是熔覆试样合金层表面显微组织。可以看出熔覆合金层由粗大的柱状晶构成，接近表面的熔覆层上有大量的

收稿日期：2007－12－26
基金项目：国家自然科学基金资助项目(50574068)

针状物析出。图 3 是熔覆试样横截面的整体显微组织。可以看出，整个试样可以分为 4 个区域：熔覆层（完全混合区）、熔合区（部分混合区）、热影响区、基体。熔覆层组织是粗大的柱状晶；熔合区内焊缝和母材的不规则结合，形成了参差不齐的锯齿状的半熔化铁素体晶粒；热影响区中母材金属发生了重结晶或不完全重结晶，因此存在明显的富铝铁素体带和少量的珠光体（图 4）。图 5 是熔敷试样合金层与基体界面的显微组织，从图 5 中可以看出熔覆层晶粒和铁基互相交错，形成了良好的冶金结合。

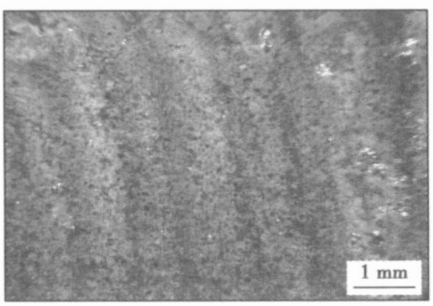

图 1 等离子熔覆试件表面成形

Fig. 1 Surface formation of plasma cladding sample

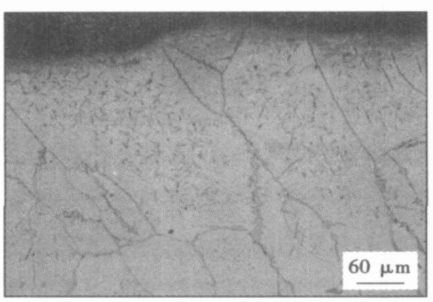

图 2 熔覆试样合金层表面显微组织

Fig. 2 Microstructure on surface of clad layer

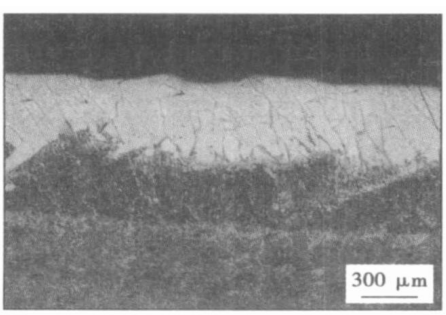

图 3 熔覆试样截面的整体显微组织

Fig. 3 Microstructure of clad cover

2.2 熔覆合金层的相构成

金相显微镜下等离子熔覆合金层由粗大的柱状晶构成，这与激光熔覆和手工氩弧堆焊的组织形态有相似之处[5,6]。表面看粗大柱状晶内有“第二相”析出，而且“第二相”的多少造成了粗大晶粒之间的明暗差异（采用醋酸硝酸水溶液腐蚀剂，其中 CH_3COOH 25 mL，HNO_3 15 mL，HCL 15 mL，H_2O 5 mL，观察金相组织可看到，晶粒之间有明暗差异，如图 6 所示）。能谱分析结果表明，明暗程度不同的粗大柱状晶之间的针状物和晶界之间成分都没有差异。图 7 为较高倍率下柱状晶团内部组织的扫描电镜像。仔细观察可以看出，这些晶粒尽管大小不等，形貌看似不同，实际均为板条状形态。造成柱状晶团之间明暗差异的主要原因可能是各个柱状晶团内部的板条晶的多少差异引起的。为进一步检测熔覆层物相构成，对熔覆层平面试样作了 X 衍射物相分析，衍射试验结果见图 8。熔覆合金层主要相是铁铝金属间化合物 Fe_3Al，FeAl 和 α-Fe 相及 Al_2O_3。由 EDS 分析可知，涂层的平均 Al 元素含量为 17%（原子分数）。Fe-Al 二元合金相图如图 9 所示[8]，可以看出，当 Al 元素含量为 17%（原子分数）时，熔体凝固后在高温时的稳定相为 α-Fe 固溶体，随着温度的降低，将发生 α-Fe→FeAl→Fe_3Al 的无序→有序转变[7]。在等离子熔覆条件下，由于熔滴内部的合金化不均匀，并使 FeAl→Fe_3Al 的转变受到抑制，从而导致在

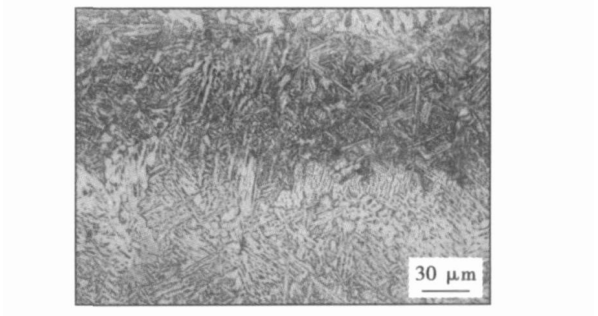

图 4 热影响区的显微组织

Fig. 4 Microstructure of HAZ

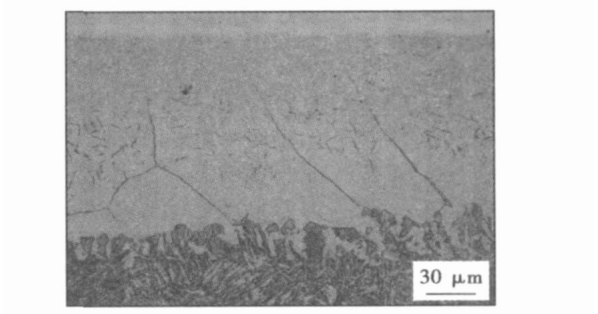

图 5 熔覆试样合金层与基体界面的显微组织

Fig. 5 Microstructure of clad-matrix interface

室温下涂层中 Fe_3Al 和 FeAl 与 α-Fe 相同时存在。同时熔覆表面还有少量的 Al_2O_3，这主要是涂层表面的铝被氧化而生成，Al_2O_3 的生成使表面形成了 Fe_3Al 金属间化合物——Al_2O_3 陶瓷涂层，增大了表面的耐磨性。

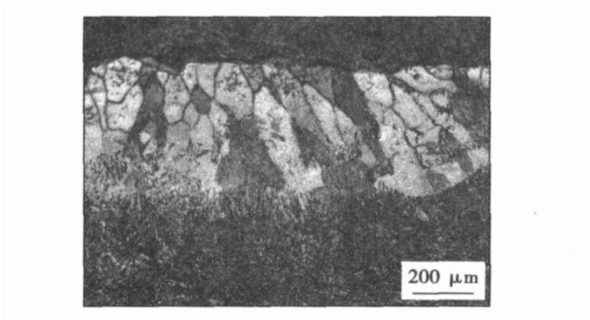

图 6　醋酸硝酸水溶液腐蚀剂的显微组织

Fig. 6　Microstructure of clad nitric-acetic acid corrosive

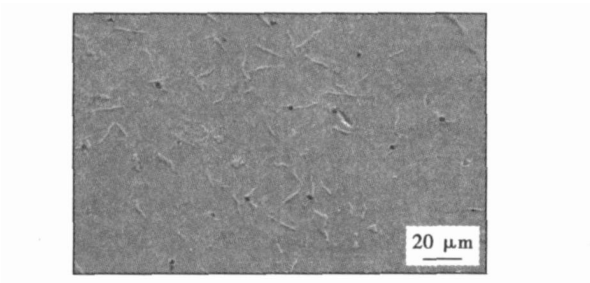

图 7　熔覆层 SEM 像

Fig. 7　SEM structure of cladded layer

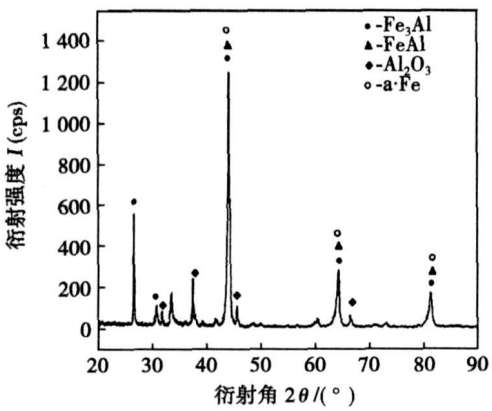

图 8　熔覆表面 X 射线衍射图谱

Fig. 8　XRD spectrum of clad layer

2.3　熔覆合金硬度

图 10 为熔覆试样测定硬度结果，从图中可以看出焊缝区的熔覆层的最外层平均硬度值为 421 HV，最高达到了 514 HV，而常规熔铸法获得的

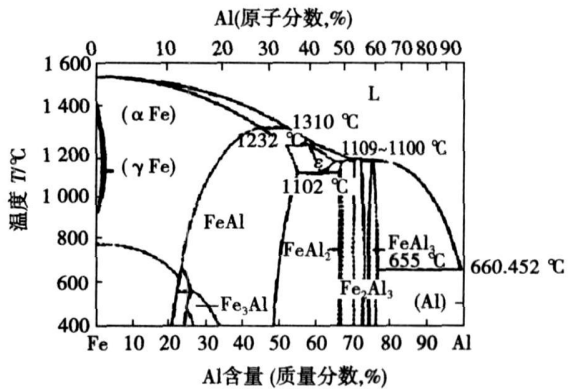

图 9　Fe-Al 二元合金相图

Fig. 9　Fe-Al binary alloy phase diagram

铸态 Fe_3Al 的硬度一般不超过 300 HV[5]。等离子熔覆 Fe_3Al 较普通铸态 Fe_3Al 硬度大大提高，一方面可能与等离子熔覆时快速加热与冷却工艺造成的应力有关，另一方面，更大程度上可能与激光熔覆工艺下形成的 Fe_3Al 合金层的特殊组织结构有关，即熔覆层事实上由大量极微细的 Fe_3Al 板条晶构成。从图中还可看出硬度值从焊缝区、熔合区到基体依次降低，大大增加了基体的硬度。

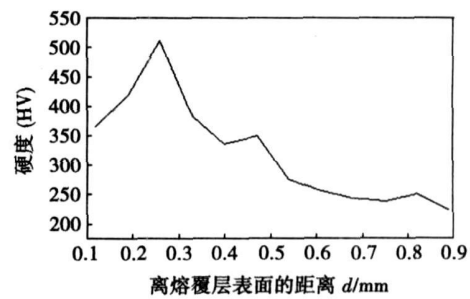

图 10　熔覆表面到基体的硬度值曲线

Fig. 10　Microhardness of clad layer to base metal

3　结　　论

（1）采用等离子熔覆方法获得了没有明显组织突变和宏观界面的 Fe-A1 金属间化合物——Al_2O_3 陶瓷涂层，涂层的组织表现出宏观不均匀性和微观连续性的分布特征。

（2）采用等离子熔覆 Fe_3Al 工艺可以在低碳钢基体的表面制备 Fe-Al 金属间化合物合金覆层。在适当熔覆工艺条件下，可以获得致密、无肉眼可见气孔、夹杂、熔覆表面有一定起伏的合金层，合金层与

[下转第 24 页]

差小于0.4 mm，能够满足实时跟踪的要求。

4 结 论

（1）传统结构光技术存在导前误差，在对不规则曲焊缝跟踪时导前误差无法用传统方法消除。

（2）双线预扫描结构光焊缝跟踪技术是在正式焊接前用两条激光线扫描焊缝并记录焊枪枪尖偏差，再在正式焊接时予以校正的技术。它能有效消除导前误差，且抗干扰能力强。

（3）建立了双线预扫描结构光焊缝跟踪技术的跟踪运动模型；提出了综合运用中值滤波、阈值变换、细化变换等技术的图像处理体系，与基于直方图的直线拟合技术，能够快速提取焊缝中心信息。

（4）为跟踪系统编制了软件，进行了小批量试验。结果表明该技术能有效克服导前误差，抗干扰能力强，计算速度快，能够满足实时跟踪的要求。

参考文献：

[1] 陈善本. 智能化机器人焊接技术研究进展[J]. 机器人技术与应用，2007(5)：8－11.

[2] 王 伟，邹奇仕，朱六姝，等. 视觉传感器焊缝跟踪技术的发展状况及实施方案探讨[J]. 电焊机，2002，32(5)：1－4.

[3] Wang Kezheng，Chen Xinzheng，Jia Gaofeng. Automatic seam tracking system of submerged arc welding based on fuzzy-p controller[J]. Chinese Journal of Mechanical Engineering，2004，17(1)：78－81.

[4] Li Liangyu，Fu Lingjian，Zhou Xin，*et al*. Image processing of seam tracking system using laser vision robot[J]. Weld，Intellige & Automation，2007，362(1)：319－324.

[5] 高向东，赵传敏，丁度坤. 图像处理技术在焊缝跟踪中的应用研究[J]. 焊接技术，2006，35(3)：3－7.

[6] 刘极峰. 机器人技术基础[M]. 北京：高等教育出版社，2007.

[7] Kuo H C，Wu L J. An image tracking system for welded seams using fuzzy logic[J]. Journal of Materials Processing Technology，2002，120：169－185.

[8] Chen S B，Chen X Z，Qiu T. Acquisition of weld seam dimensional position information for arc welding robot based on vision computing [J]. Journal of Intelligent and Robotic Systems，2005，43：77－97.

[9] Bridge E W. Practical techniques to improve arc welding robot cell use[J]. Robotics Today，1995，8(1)：1－6.

[10] Kim J S，Song Y K，Cho H S，*et al*. A robust visual tracking system for robotic arc welding systems[J]. Mechatronics，1996，6(2)：141－163.

作者简介：肖增文，男，1970 年出生，博士，讲师。主要从事智能机器人以及焊接技术的科研和教学工作。发表论文 30 余篇。

Email：x_zwen@163.com

[上接第 19 页]

基体间实现了良好的冶金结合。

（3）熔覆合金层主要由铁铝金属间化合物 Fe_3Al，FeAl 和 α-Fe 相及 Al_2O_3 构成，覆层组织由粗大的柱状晶团构成。柱状晶团内包含大量极细小的板条状 Fe_3Al 晶粒。

（4）熔覆合金层的最高显微硬度可达到 514 HV。

参考文献：

[1] 陈国良，林均晶. 有序金属间化合物结构材料[M]. 北京：冶金工业出版社，1999.

[2] Mckamey C G，Devan J H，Tortorelli P T，*et al*. A review of recent developments in Fe_3Al-based Alloys[J]. Journal of Material Research，1991(6)：1779.

[3] 徐滨士，朱子新，刘 燕，等. 高速电弧喷涂 Fe-Al 金属间化合物涂层[J]. 中国有色金属学报，2004(14)：154－158.

[4] 陈 瑶，王华明. 激光熔覆 TiC 增强 Fe_3Al 金属间化台物基复合材料涂层磨损性研究[J]. 稀有金属材料与工程，2003，32(10)：840－843.

[5] 尹衍升，施忠良，刘俊友. 铁铝金属间化合物[M]. 上海：上海交通大学出版社，1996.

[6] 程广萍，何宜柱. 钢基表面单道激光熔覆 Fe_3Al 金属间化合物的研究[J]. 铸造技术，2004，25(8)：600－601.

[7] Du G W，Wang Z，Xiao J M. Phase transformations in Fe-28Al alloys [J]. Acta Metallurgical Sinica，1995，31(4)：A151－A155.

[8] Liu Z，Gao W，Wang F. Oxidation behavior of FeAl intermetallic coatings produced by magnetron sputter deposition[J]. Scripta Materilla，1998，39(11)：1497－1502.

作者简介：朱冬妹，女，1978 年出生，硕士研究生，工程师。主要从事焊接冶金和表面工程方面的研究工作。发表论文 5 篇。

Email：zhusanmei1979@126.com

MAIN TOPICS, ABSTRACTS & KEY WORDS

Arc assisted activating TIG welding process FAN Ding[1,2], LIN Tao[2], HUANG Yong[1,2], NIU Shufeng[2] (1. State Key Laboratory of Gansu Advanced Non-ferrous Metal Materials, Lanzhou University of Technology, Lanzhou 730050, China; 2. Key Laboratory of Non-ferrous Metal Alloys, The Ministry of Education, Lanzhou University of Technology, Lanzhou 730050, China). p1—4, 32

Abstract: A new activating welding process, arc assisted activating TIG welding (AA-TIG welding), is put forward. The effects of welding parameters on weld penetration and width are studied using SUS304 stainless steel as base metal. The results indicate that the weld penetration of AA-TIG welding can increase above 2 times of that of the traditional TIG welding in the same welding conditions and the weld width reduce dramatically. Using AA-TIG welding process, the 8mm thickness stainless steel can be fully penetrated without making a groove. Welding efficiency is obviously improved. Welding specifications of the assisted arc and common TIG welding have influence on the weld penetration and width of AA-TIG welding.

Key words: stainless steel; AA-TIG welding; carbon dioxide; weld appearance

Stability of CO_2 GMAW with short-circuit transfer based on Lyapunov exponent CAO Biao, XIANG Yuanpeng, ZENG Min, HUANG Shisheng (College of Mechanical Engineering, South China University of Technology, Guangzhou 510641, China). p5—7, 16

Abstract: Based on the experimental time series of welding current produced by carbon dioxide gas metal arc welding (CO_2 GMAW) with short-circuit transfer under different welding speeds, the largest Lyapunov exponents of the welding system are numerically evaluated using Takens' phase space reconstruction technique and the Wolf's algorithm for Lyapunov exponent. The results show that the largest Lyapunov exponent reaches small values when the welding processes approach high steady states. While the system is at the unsteady mode and experiences rapid variation, the largest Lyapunov exponent attains large values. So the largest Lyapunov exponent is negatively correlated with the welding process stability and can be taken as a novel indicator to quantify the process stability of CO_2 GMAW with short-circuit transfer.

Key words: CO_2 GMAW; welding current; Lyapunov exponent

Interphase diffusion-solution zone of Al/Co SONG Yuqiang, LI Shichun, YANG Zeliang (College of Mechanical and Electronic Engineering, China University of Petroleum, Dongying 257061, China). p8—12

Abstract: By using diffusion couple made by inlaying, the diffusion-solution zone of Al/Co was researched under different anneal conditions. The microstructure and forming rule were observed and analyzed by means of SEM and EDS, and its forming mechanism was discussed. The results show that the diffusion-solution zone is formed at Al/Co interphase when heating temperature 600 ℃ and holding time 75 hours, its thickness is 170 μm, and its structure is Al/Co_2Al_9/Co_4Al_{13}/Co_2Al_5/CoAl/Co, the structure being consistent with sequence of each phase in Al/Co binary alloy phase diagram. CoAl phase layer is firstly formed on Co, and other three layers are then formed on CoAl; the Co_4Al_{13} phase layer and Co_2Al_5 phase layer grow with the opposite direction in "pole pattern", they turn around landscape orientation to grow from root after they have developed definite thickness, and layer 2 and layer 3 intervene in tow; lastly, Co_2Al_9 phase layer is formed at Al/Co_4Al_{13} interface. The forming of Al/Co diffusion-solution zone resulted from diffusion, dissolve and crystal of Al and Co under the condition of solid phase. The reciprocity of concentration and solubility caused the formation sequence of diffusion-solution zone.

Key words: Al; Co; diffusion welding; interphase; diffusion zone

Microstructure simulation in welding 1Cr18Ni9Ti steel ZHAO Yuzhen[1], ZHAO Haiyan[2], SHI Yaowu[3] (1. Department of Materials Science and Engineering, Tsinghua University, Beijing 100084, China; 2. Department of Mechanical Engineering, Tsinghua University, Beijing 100084, China; 3. School of Materials Science and Engineering, Beijing University of Technology, Beijing 100022, China). p13—16

Abstract: The growth of columnar grain during the solidification of the 1Cr18Ni9Ti stainless steel weld metal for different welding parameters is simulated using the grain boundary evolution (GBE) modeling method. The shape and the size of the weld pool under different welding parameters are calculated using PHOENICS software. The simulated results show that the growing direction of the columnar grains is dependent on the shape of the weld pool. The straight and short grains tend to grow in direction perpendicular to the weld centerline if the length/width (L/W) of the weld pool is large and the curving and long grains grow toward the welding direction if the L/W ratio is small. The experimental results are found to be in good qualitative agreement with the simulated results.

Key words: grain boundary evolution model; structure simulation; weld solidification; stainless steel

Mcrostrueture of Fe_3Al intermetallic compound produced by plasma cladding ZHU Dongmei[1,2], WANG Xibao[1] (1. Beijing Xinghang Mechanical-Electric Equipment Plant, Beijing 100074, China; 2. School of Material Science and Engineering, Tianjin Uni-

versity, Tianjin 300072, China). p17—19, 24

Abstract: Arc spraying and plasma cladding process was used to prepare the aluminum composite coating. The microstructure and phase structures of the clad alloy layer and the interface of alloy layer and steel matrix composites were analyzed. The results show that the tight alloy layer without pore and inclusion is obtained, and the coating and the steel are metallurgically compacted. The clad alloy layer consists of phase Fe_3Al, FeAl, α-Fe and Al_2O_3. Microhardness of the clad alloying layer will be 514 HV.

Key words: plasma cladding; Fe_3Al; intermetallic compound

Application of pre-scanning technology with laser to seam-curved tracking XIAO Zengwen, LIU Jifeng, CHEN Zhichao, GONG Xun (Department of Mechanical Engineering, Nanjing Institute of Technology, Nanjing 211167, China). p20—24

Abstract: The structured-light technology of traditional seam tracking makes front guiding error great if the curvature is varying. To solve the problem, a structured-light pre-scanning technology with double lines is produced. The seam is scanned before welding along the planned track of the robot. A laser line is added under the welding torch tip to indicate the front guiding error that will be recorded on time sequence and be eliminated when welding. A seam tracking system and its mathematical model are established. An image processing system is advanced, which the integrations of image processing technologies including median filtering, threshold transforming, thinness transforming and subsection beeline fitting locate the seam middle exactly. Tests show that the technology combined with the image processing system has the characteristics of strong anti-jamming, little error and fast processing speed, and it can meet the request of real time tracking.

Key words: seam tracking; structured-light; pre-scanning; image process; curved seam

Microstructure and shear strength of diffusion brazed Al_2O_3-TiC/Q235 joint WANG Juan[1], LI Yajiang[1], S. A. GERASIMOV[2] (1. Key Laboratory of Liquid Structure and Heredity of Materials, Shandong University, Jinan 250061, China; 2. Materials Science Department, Bauman Moscow State Technical University, Moscow 105005, Russia). p25—28

Abstract: An Al_2O_3-TiC/Q235 joint, Al_2O_3-TiC ceramic composite with steel Q235, was obtained by diffusion brazing in vacuum, using a combination of Ti and Cu as multi-interlayer. The interfacial strength was measured by shear testing and the result was explained by the fracture morphology. Microstructure of the Al_2O_3-TiC/Q235 joint was investigated by scanning electron microscope (SEM), energy-dispersion spectroscopy (EDS) and X-ray diffraction (XRD). The results indicate that the Al_2O_3-TiC/Q235 joint with a shear strength of 122 MPa can be obtained by controlling heating temperature at 1 110 ℃, multi-interlayer Ti/Cu/Ti is fused fully and diffused reaction to produce an obvious interfacial transition zone with a thickness of about 80 μm, and there are Ti_3AlC_2, Fe_2Ti, Cu and TiC in the transition zone.

Key words: Al_2O_3-TiC; diffusion brazing; shear strength; microstructure

Cross-section modeling of weld bead for rapid prototyping by MAG welding based on wavelet transform CAO Yong, ZHU Sheng, SUN Lei, SHEN Canduo, LIANG Yuanyuan, WANG Wanglong (National Defense Key Laboratory for Remanufacturing, Academy of Armored Forces Engineering, Beijing 100072, China). p29—32

Abstract: A new modeling method of weld bead profile by MAG welding process was proposed and the edge of the profile was extracted based on wavelet transform. The different interpolation methods, the cubic spline, the constrained cubic spline and the B-spline curve, were utilized respectively, the cross-section edge of weld bead was fitted by least square method, and then the mathematical model of the profile was achieved. The experimental results show that the method is effective to detect the cross-section outline of the profile, the constrained cubic interpolation is preferred choice to interpolate the data of the profile, and the cross-section profile mathematical model of weld bead is sine curve under our experiments.

Key words: rapid prototyping; wavelet transform; edge detection; modeling

Microstructure and wear resistance of plasma cladding Al_2O_3+TiO_2/Fe alloy composite coating LU Jinbin, LIANG Cun, PENG Zhuqin, ZHANG Zhaojun (College of Material and Chemical Engineering, Zhongyuan University of Technology, Zhengzhou 450007, China). p33—36

Abstract: Plasma cladding Ni-Cr-B-Si-Fe-based alloy coating and Fe-based alloy composite coating with Al_2O_3+TiO_2 were obtained on the Q235 substrate, and microstructure, microhardness and wear resistance of the two coatings were investigated contrastively. The results show that the interface solidification form of Fe-based alloy composite coating with Al_2O_3+TiO_2 have changed. They become small dendrite from primary lathy dendrite, and offer core for solidification. The microstructure is mainly based on γ-Fe with fine particles, and its microhardness can reach 600~655 HV0.2.

Key words: plasma cladding; microhardness; wear resistance; Al_2O_3+TiO_2

Data collecting system of pipe arc acoustic emission characteristics LIU Lijun[1,2], LAN Hu[1], DUAN Hongwei, WEN Jianli[1] (1. School of Material Science & Engineering, Harbin University of Science and Technology, Harbin 150080, China; 2. Ningbo Institute of Technology, Zhejiang University, Ningbo 315100, China). p37—40

Abstract: As the arc sound signal contains plenty of welding information which is an important source signal for welding quality control, arc acoustic emission signal (AAES) propagated in pipeline structure is low-noise, and AAES collecting system is designed for pipe TIG welding. The hardware system consists of sensor, signal adaptor circuit, data collecting card and industrial workstation. Based on virtual instrument programming software (LabVIEW), the high speed AAES collecting software system is designed by means of triggering interrupt, packaging function modules and calling dynamic